NIH Public Access
Author Manuscript
Trends Biotechnol. Author manuscript; available in PMC 2011 July 1.

Published in final edited form as:
Trends Biotechnol. 2010 July ; 28(7): 363–370. doi:10.1016/j.tibtech.2010.04.002.

^{19}F MRI for quantitative *in vivo* cell tracking

Mangala Srinivas[1], **Arend Heerschap**[2], **Eric T. Ahrens**[3], **Carl G. Figdor**[1], and **I. Jolanda M. de Vries**[1,*]

[1]Department of Tumor Immunology, Nijmegen Centre for Molecular Life Sciences, Radboud, University Nijmegen Medical Centre, Postbox 9101, 6500 HB Nijmegen, Netherlands [2]Department of Radiology, Nijmegen Centre for Molecular Life Sciences, Radboud, University Nijmegen Medical Centre, Nijmegen, Netherlands [3]Department of Biological Sciences and the Pittsburgh NMR Center for Biomedical Research, Carnegie Mellon University, PA, USA

Abstract

Cellular therapy, including stem cell transplants and dendritic cell vaccines, is typically monitored for dosage optimization, accurate delivery and localization using non-invasive imaging, of which magnetic resonance imaging (MRI) is a key modality. ^{19}F MRI retains the advantages of MRI as an imaging modality, while allowing direct detection of labelled cells for unambiguous identification and quantification, unlike typical metal-based contrast agents. Recent developments in ^{19}F MRI-based *in vivo* cell quantification, the existing clinical use of ^{19}F compounds and current explosive interest in cellular therapeutics have brought ^{19}F imaging technology closer to clinical application. We review the application of ^{19}F MRI to cell tracking, discussing intracellular ^{19}F labels, cell labelling and *in vivo* quantification, as well as the potential clinical use of ^{19}F MRI.

Introduction

Cellular therapeutics is the transfer of cells to a patient to treat a disease or condition; for example, dendritic cells (DCs) can be used to stimulate the immune system against tumors, or stem cell transfers can restore function to damaged tissues. It is a growing field that includes islet grafts, DC vaccines, and regulatory T cell and stem cell transplants. While these treatments are promising, the technology is still in its infancy. For successful cellular therapy, it is essential that we monitor transferred cells post-transplant non-invasively, longitudinally and quantitatively using *in vivo* imaging techniques.

In vivo imaging techniques that are applicable to humans can broadly be classified based on whether or not they use radioactive nuclides. Those that use radioactive nuclides include scintigraphy, positron emission tomography (PET) and single photon emission computed tomography (SPECT), while computed tomography (CT) relies on the use of ionizing radiation. The major advantages and disadvantages of each imaging modality are described elsewhere [1]. Briefly, magnetic resonance imaging (MRI) and ultrasound are the main imaging

© 2010 Elsevier Ltd. All rights reserved.

*Corresponding author: de Vries, I.J.M. (J.deVries@ncmls.ru.nl).

Publisher's Disclaimer: This is a PDF file of an unedited manuscript that has been accepted for publication. As a service to our customers we are providing this early version of the manuscript. The manuscript will undergo copyediting, typesetting, and review of the resulting proof before it is published in its final citable form. Please note that during the production process errors may be discovered which could affect the content, and all legal disclaimers that apply to the journal pertain.

Disclosure statement
Eric T. Ahrens serves as a consultant to Celsense, Inc.

NIH-PA Author Manuscript
NIH-PA Author Manuscript
NIH-PA Author Manuscript

NIH-PA Author Manuscript

NIH-PA Author Manuscript

NIH-PA Author Manuscript

modalities that do not use radionuclides or ionizing radiation. Ultrasound imaging provides excellent real-time images, but the resolution is generally too low for cell tracking, in addition to other limitations, such as a restricted field-of-view and relatively poor tissue contrast. MRI is capable of high resolution imaging with excellent inherent soft tissue contrast, and is well-suited for longitudinal, non-invasive imaging as it does not rely on probes with short half-lives.

The utility of MRI for cell tracking in DC vaccines was demonstrated in melanoma patients [2]. This study found that the DCs were often mis-injected, being delivered outside the targeted lymph node, even with ultrasound-guided injections. This was a crucial finding, as it showed that data from studies requiring targeted, localized delivery might not be reliable. Recent reviews cover the use of MR-based cell tracking in both clinical [3] and preclinical settings [4]. In this review, we will focus on MRI for quantitative cell tracking through the use of fluorinated (^{19}F) labels.

^{1}H MRI

Contrast agents (Box 1) function by modifying the ^{1}H signals from the huge amount of mobile water in tissues (~50 M). Contrast can also be generated through the modulation of intracellular metalloprotein levels through gene therapy [5]. The minimum detectable concentration of a contrast agent is dependent on the extent to which the agent modifies local nuclear magnetic resonance (NMR) relaxation rates, typically micro- or millimoles per voxel. However, because these agents only modify contrast in an image, unambiguous localization can be difficult, as shown in Figure 1; thus, “before” and “after” images are often required in order to detect the contrast agent *in vivo*. This requirement for repeated imaging sessions can be challenging in animal models, but it can be even more difficult clinically due to patient welfare, scheduling and monetary concerns. Localization based on contrast modulation is further complicated by intrinsic sources of contrast in tissues, such as blood clots, deoxyhemoglobin, inflammation and endogenous iron. Localization can be especially difficult when hemorrhage is present due to the high iron content. Furthermore, quantification of agent concentration in a region of interest (ROI) can be difficult, as it is affected by several factors, including a non-linear relationship between concentration and relaxation constants [6] and a strong reliance on the imaging sequence and parameters used. However, it is possible to detect superparamagnetic iron oxide (SPIO) more accurately using more advanced techniques, such as phase mapping or “white marker” techniques [7], although these techniques may be difficult to apply in humans because of safety concerns regarding imaging sequences with multiple high-energy pulses. Lastly, heavy metal contrast agents can be toxic [8], particularly to patients with pre-existing kidney disease [9]. Table 1 summarizes key properties of current cell labels.

For all these reasons, there is increasing interest in the development of a “second color” or “hot-spot” imaging – heteronuclear MRI using ^{13}C, ^{23}Na, ^{31}P, or ^{19}F, in addition to ^{1}H. The use of these nuclei enables direct detection rather than the indirect detection necessary for contrast agents, thus avoiding the need for pre-scans and removing localization ambiguity. ^{13}C, ^{23}Na, and ^{31}P are used extensively in MR spectroscopy, although there is a loss of sensitivity because the concentration and gyromagnetic ratio of these elements are much lower than that of ^{1}H. All of these isotopes are naturally present in biological tissues, which can add to the background signal. By contrast, there is no detectable background in tissues for ^{19}F NMR or MRI.

^{19}F MRI and perfluorocarbons

^{19}F MRI has been demonstrated for over 20 years [10], with the first *in vitro* study of ^{19}F NMR image formation or “zeugmatography” in 1977 [11]; this study also suggested the use of ^{19}F compounds as “tracers” in a sample. ^{19}F has several properties that make it suitable for use as an MRI tracer: (i) a high relative sensitivity that is 83% of ^{1}H; (ii) 100% natural abundance;

NIH-PA Author Manuscript

NIH-PA Author Manuscript

NIH-PA Author Manuscript

(iii) its resonance differs by only 6% from that of ^{1}H, potentially allowing one to conduct ^{19}F MRI on existing ^{1}H imaging hardware; (iv) an extremely broad chemical shift and a T_1 sensitivity to oxygen tension that might permit its use as an *in vivo* sensor; (v) not naturally present in biological tissues and therefore does not contribute to background signal (fluorides in bone and teeth have exceedingly short T_2 values and thus do not add background); and (vi) perfluorocarbons (PFCs) have been extensively studied as blood substitutes, and, as such, the biodistribution and toxicity of these compounds is known.

PFCs have been used widely *in vivo*, including as contrast agents for imaging modalities other than MRI. A recent review on PFCs in clinical imaging highlights their use in ultrasound imaging as a vehicle for targeted delivery of contrast agents and drug delivery [12]. PFC microbubbles have been employed for labeling specific blood cells for ultrasound detection [13] and as tumor-targeting drug carriers [14]. Dual-mode agents for ultrasound and ^{19}F MRI have also been reported [15]. PFC nanoparticles have been used for improved characterization of liver lesions in a late phase clinical trial using CT [16], and in eye surgery due to their high density and inertness, although not as an imaging agent [17]. Fluorinated compounds other than PFCs are used as drugs and anesthetics.

PFCs have also been widely employed within the field of MRI. The inertness of the compounds allows them to withstand harsh emulsification procedures and nanoparticle formulations, and to act as nonreactive carriers for other compounds, chiefly drugs. For example, PFC nanoparticles have been suggested for “contact-facilitated” drug delivery [18] and ^{19}F MRI can be used for non-invasive dosimetry of drugs [19]. The oxygen sensitivity of the ^{19}F T_1 relaxation rate of some PFCs has similarly been exploited: PFC-loaded alginate capsules were implanted *in vivo* in rats for over three months to monitor oxygen partial pressure [20]. Oxygen tension has been measured in lungs using PFC aerosols [21]. Other applications include a PFC encapsulated in chemical exchange saturation transfer (CEST) liposomes for temperature-sensitive drug release for both quantification via ^{19}F MRI and CEST contrast [22]. Magnetic resonance spectroscopy (MRS) and NMR have also been used widely with ^{19}F compounds, because of the large chemical shift range of ^{19}F. For example, quantitative enzyme activation studies, where a fluorinated substrate is differentiated from the end product by a change in chemical shift using ^{19}F, have been carried out with MRS [23]. ^{19}F NMR has also been applied to the study of gene expression [24]. Generally, all the above uses are possible, or vastly simplified, by the absence of ^{19}F background *in vivo*. Taken together, these studies demonstrate the versatility of fluorinated compounds, and the breadth of research that has already gone into their use *in vivo.* Furthermore, the ability to detect some PFCs through more than one imaging modality also opens up possibilities for *in vivo* multimodal imaging applications. General requirements for a ^{19}F label are outlined in Box 2, and ^{19}F label formulation for cellular MRI is discussed in Box 3.

Cell labeling

Cells can be labeled *in situ* or *ex vivo* before transfer to the subject. *In situ* labeling typically involves the nonspecific uptake of intravenous tracers by phagocytes, mainly macrophages [25]. Alternatively, the agent may be targeted to specific cells using antibodies [26-28], or the label is injected directly into the tissue of interest [29]. However, *ex vivo* labeling is the most commonly used technique for tracking a specific group of cells because it results in reproducible and uniform labeling.

Cell labeling using contrast agents, including iron oxide particles of sizes ranging from several nanometers to micrometers, can be challenging, especially for non-phagocytic cells due to poor cell loading. Techniques utilizing transfection agents [30,31], electroporation [32], peptide incorporation [33], and receptor-mediated uptake [34,35] have been used. PFC emulsions can

NIH-PA Author Manuscript

NIH-PA Author Manuscript

NIH-PA Author Manuscript

be formulated for cell uptake using various techniques, including the use of transfection agents to impart a positive charge to the droplets [36,37], or by adding charged lipids to the surfactant mix [38]. However, even non-phagocytic cells (T cells and neuronal stem cells) have been labeled with anionic or cationic ^{19}F emulsions without the need for added transfection agents [38,39]. This is important, as most transfection agents are not approved for clinical use. Box 3 describes general strategies for ^{19}F cell label formulation using PFCs.

In general, quantitative cell labeling studies using ^{19}F emulsions have resulted in a cell loading of 10^{11}-10^{13} ^{19}F atoms per cell [36,37,39,40], with the levels typically higher in phagocytic than non-phagocytic cells. Human DCs labeled with a ^{19}F agent showed no significant changes in viability, phenotype or functionality when used in cell vaccination studies [41]. The uptake of 10^{12}-10^{13} ^{19}F atoms per cell results in a minimum detection sensitivity of approximately 2000 cells/voxel at 7 T *in vitro*. The detection limit in patients receiving SPIO-labeled dendritic cells was shown to be 1000 cells/mm^3 at 3 T [42]. While the sensitivity of imaging is dependent on many factors other than just cell loading, this comparison allows a rough estimation of the detectability of ^{19}F-labeled cells relative to cells labeled with contrast agents. However, note that imaging with ^{19}F agents can be about 10-fold slower than with contrast agents, and this is a major disadvantage of the technique.

Finally, it should be noted that current MR labels for cell tracking do not change with respect to cell death or functionality. Instead, we only detect the presence or absence of label in the image and must then make the assumption that the label remains associated with the relevant cells. The validity of this assumption can be verified using conventional assays and histology *ex vivo* to examine the localization of the label within the cells and tissue. Labeled neuronal stem cells were found to remain viable, without leakage or transfer or label, for at least two weeks after transfer to the brain in mice [38]. Furthermore, ^{19}F label is retained within the cell and divided between daughter cells during cell division, at least with murine T cells [39]. Thus, although the long-term fate of ^{19}F labels is not known, it appears that they are suitable for cell tracking up to at least 2-3 weeks post-cell transfer. Cell tracking with non-dividing, non-migratory cells may be possible for extended lengths of times.

In vivo imaging

The key factor that needs to be maximized for imaging using ^{19}F MRI is the signal-to-noise ratio per unit time (SNR/t). For ^{19}F MRI, this translates to the use of fast imaging sequences, sensitive hardware and high magnetic field strength. Generally, it is sufficient to detect the presence or absence of ^{19}F signal in an ROI, and therefore high-resolution is typically not required.

Signal strength in NMR is affected by several factors, including hardware (e.g. coil design and its filling factor), image acquisition parameters (e.g. imaging sequence and number of averages), gyromagnetic ratio (γ) of the nucleus being imaged, magnetic field strength, temperature, and nuclei (spin) density. Of these parameters, hardware and imaging parameters are beyond the scope of this review. The choice of ^{19}F nuclei results in a large γ, which is comparable to that of ^{1}H. The field strength is generally fixed (by the magnet at hand), as is temperature (by the body). Thus, only the spin density can be varied. This value is dependent on label uptake per cell and the distribution of labeled cells *in vivo* – in other words, whether the cells are dispersed, as in the blood, or concentrated, as in lymph nodes. *In vivo* ^{19}F MRI studies in mice have shown that a minimum of 7500 labeled cells/voxel is required for detection at 11.7 T using a rapid acquisition with relaxation enhancement (RARE, also known as turbo spin echo or fast spin echo) imaging sequence, when the cells contained 10^{13} ^{19}F atoms per cell (a dose of 0.1g/kg of ^{19}F via the labeled cells) [37]. It is worth noting that voxels can be enlarged to increase the number of labeled cells contained within. Cells localizing at densities

NIH-PA Author Manuscript

NIH-PA Author Manuscript

NIH-PA Author Manuscript

below the detection limit as well as cells in motion, such as cells in circulation, will not be detected.

Fast imaging sequences are necessary for optimizing SNR/t. Research on fast MRI is ongoing and there are many approaches to this complex topic, including restricted k-space acquisition, compressed sensing algorithms for fast acquisition [43] and innovative sequences. Fast imaging has been applied to ^{19}F imaging, for example using fast imaging sequences like fast low angle shot (FLASH), fast low angle rapid acquisition with relaxation enhancement (FLARE), and RARE (or fast spin echo) [44-49]. A key concern toward clinical applicability of fast imaging sequences is the specific absorption rate (SAR) deposition. SAR is the radio frequency (RF) power absorbed per unit mass of the subject during MRI (W/kg). This energy can result in heating, and the effect is often localized. SAR can become too high, especially with sequences using multiple pulses and short repetition times, or at high field strengths. SAR values well above clinical restrictions can result in significant temperature increases in tissues, effectively limiting use in humans [50,51].

Cell number quantification

Cell number quantification *in vivo* requires accurate knowledge of the amount of label per cell (L_c) prior to cell transfer. L_c can be determined by measuring the total ^{19}F content in a known number of cells [36] *in vitro* using a simple NMR measurement. In this measurement the spectral weight of the label in a cell pellet is compared to a known concentration of a ^{19}F reference compound added to the sample having a different value of chemical shift [36,37, 39,52,53]. This technique can additionally be applied *ex vivo* to excised tissue using ^{19}F NMR for more sensitive quantification [37]. L_c may change over time due to cell division or loss of label from the cells, and thus should be verified in cells in *ex vivo* culture where possible. Furthermore, MRI is not sensitive to whether the label is transferred or lost to other cells, such as macrophages in the vicinity, or even to the extracellular matrix. However, this is an issue with cell labels in general and is not restricted to MRI tracers.

Quantification can also be carried out directly from the *in vivo* ^{19}F image data [37,39], which is a slightly more complex process (Figure 2). ROIs are selected surrounding reference, cellular, and background (outside the subject) signals. The reference consists of a sealed tube with a known concentration of the label placed within the field of view. ROI selection can be performed with the aid of anatomical data from the ^{1}H scans. A mask is applied to automatically select voxels containing a signal greater than the corrected noise value with 99% certainty. The mask is then dilated by one-half a voxel in-plane in order to correct for any partial volume effects. Total signal in the ROI is then calculated automatically, after correction for signal due to non-Gaussian noise at low SNR values. The total signal in the ROI is then divided by the L_c to estimate the number of cells. This technique proved highly accurate with *in vitro* cell phantoms ranging from 0.75-12×10^4 cells/voxel [37]. The accuracy of the calculated cell number is dependent upon the accuracy of L_c, which may change over time due to cell division or loss of label. Nevertheless, this technique has been applied up to 21 days post-cell transfer with rapidly dividing T cells [39].

Noise in MR images generally results from thermal radiation from the subject and random electrical fluctuations in the hardware. Due to the nature of MRI acquisition, noise occurs over the whole magnitude image, and its distribution is Rician or Gaussian, depending on the SNR of the image. The SNR itself is proportional to the square root of the number of acquisitions; thus, noise correction is necessary at low SNR values. To reduce bias in the calculated signal due to non-Gaussian noise at low SNR values using the quantification technique described above, the noise intensity was calculated on a per-voxel basis by estimating the value of the noise in the magnitude image based on a distribution calculated in the complex data. The

NIH-PA Author Manuscript

NIH-PA Author Manuscript

NIH-PA Author Manuscript

process was done on a per-voxel basis to account for the signal dependence of the noise intensity. Noise correction is not perfect; however, the average noise value is closer to zero after correction.

In vivo quantification using ^{19}F MRI with short repetition times can be susceptible to oxygen partial pressure values; some PFCs are used as oxygen sensors because their T_1 changes with oxygen content (reviewed in [54]). This can affect the perceived total signal in an ROI. However, linear PFCs are generally less sensitive to oxygen partial pressure and therefore can be more suitable for quantification [37,39].

Translation to the clinic

MRI is currently used extensively in humans, even in pregnant women, when conventional ultrasound scans are insufficient [55]. The risks involved arise from the strong, static magnetic field of the imaging system, which can turn common clinical tools (i.e. oxygen tanks or scissors) into deadly projectiles, and the pulsing RF 3-7 T is considered “high field” for clinical MRI, although current cell tracking studies using ^{19}F MRI in mice have typically been at higher field strengths. Nevertheless, even when imaging at an ultra-high field strength (e.g. 11.7 T) without SAR restrictions on the choice of imaging sequences, and with less restrictions on acquisition times, the SNR of the ^{19}F images obtained in animal studies is often just above the detection threshold. Thus, is it reasonable to expect clinical success of ^{19}F MRI for human patients?

In fact, some clinical studies may be well-suited for cell tracking using ^{19}F MRI. Cell transfer trials in humans often use large numbers of cells, on the order of tens of millions, transferred locally (e.g. intranodally, subcutaneously or as a graft). Such trials may be more amenable to ^{19}F MRI because of the dense localization of the cells resulting in a high cell density per voxel. Systemic cell transfers may be more challenging as the label may not accumulate locally at sufficient concentrations for imaging (i.e. the number of cells/ voxel may not cross the detection threshold). However, since the ^{19}F images are overlaid on high resolution ^{1}H anatomical scans, the resolution and SNR of the ^{19}F images can be much lower, thus increasing the numbers of cells per voxel over the detection limit. Another intriguing approach to overcome the low sensitivity of MRI is the use of hyperpolarized agents, which are capable of producing an astounding 10,000-fold increase in the SNR. Using hyperpolarized ^{3}He, Tsai and colleagues were able to image a breath-hold human lung [56]. The technique has not yet been applied to cell tracking due to the short lifetimes of hyperpolarized agents and the harsh conditions needed for their generation. However, hyperpolarization technology is progressing rapidly, being applied to ^{13}C for *in vivo* metabolite tracking, for example [57,58]. The short lifetimes of hyperpolarized agents makes the application to longitudinal cell tracking difficult, but the technique holds great promise.

Another important concern relating to clinical use is the fate of PFCs in the system. In fact, PFC clearance from biological systems is well-studied due to their prior use as surgical blood substitutes. Note that the PFC dose delivered in intracellular labels is several orders of magnitude smaller than for artificial blood substitutes. In general, smaller PFCs are lost through exhalation from the lungs due to their low vapor pressures, whereas higher molecular weight PFCs are cleared by the reticuloendothelial system. In all cases, there is no evidence for metabolic by-products of the compounds, thus indicating that the PFCs are not broken down *in vivo*, which limits the possibility of reactive intermediate formation [59,60]. This is not surprising, as the C-F bond is extremely strong, and there are no known enzymes that can attack it. A study in rats that received an intravenous administration of 3.6 g/kg of fluorocarbon emulsion found that 70% accumulated in the liver after 24 hrs, with the remaining fluorocarbon predominantly located in the spleen, with small amounts in the lungs, kidneys and blood, and no evidence of metabolism. The half-time for this particular fluorocarbon with this route of

NIH-PA Author Manuscript

NIH-PA Author Manuscript

NIH-PA Author Manuscript

delivery was found to be ~25 days [61]. While it may be difficult to extrapolate the fate of other PFCs from this study, it does provide a general idea of the persistence of the compounds *in vivo*. A study tracking PFC-labeled T cells *in vivo* in mice, saw the ^{19}F signal decrease significantly after about three weeks [39]. This could reflect emigration of labeled cells from the region of interest or clearance of label from dead cells. In either case, it suggests that clearance of label from the ROI may not be a problem.

Unfortunately, certain PFCs are now ubiquitous in the environment as pollutants. Perfluorooctanesulfonate and perfluorooctanoate accumulate in humans all over the world, and have been detected in blood, internal organs and even breast milk. Various epidemiological studies have shown inconsistent data linking these PFC compounds with postnatal development in infants, although studies in rats and mice suggest a stronger effect (reviewed by [62]). However, the applicability - if any - of toxicity data from studies on perfluoroalkyl pollutants to PFC blood substitutes or imaging agents is minimal, given the differences in chemical structure, dosage, route of delivery and length of exposure time.

Concluding remarks

^{19}F MRI for cell tracking is still in an early stage of development. The main hurdle facing this technology is sensitivity (i.e. detection of ^{19}F tracers within a reasonable time frame to allow clinical use). However, the technology is actively being researched from multiple angles, including imaging hardware, imaging sequences, label development and cell labeling. It is an exciting multi-disciplinary field involving chemistry, biology, medical research, physics and engineering. The breadth and depth of the progress made over the last few years are not only proof of the potential of ^{19}F MRI, but also indicators of a large-scale desire for its continued maturation and clinical application.

Box 1. Contrast agents in MRI

Initial contrast agents and ^{19}F formulations were not specifically designed for intracellular labeling, but rather for blood pool or lesion contrast. The intrinsic contrast observed in MR images depends heavily on the spin density and relaxation times. In ^{1}H MRI, the spin density is governed by the concentration of mobile water in tissues and is therefore not a variable *in vivo*. MR contrast agents are classified as either T_1 or T_2 (or T_2*) agents; T_1 agents result in hyperintensity, and T_2 (or T_2*) agents in hypointensity (Table 1). Contrast agents are not detected directly, but instead through their effects on the intrinsic ^{1}H signal (i.e. their effect on local water relaxation rates). Given the high concentration of ^{1}H from mobile water, *in vivo* detection of contrast agents can be very sensitive.

T_1 agents

T_1 is the longitudinal or spin-lattice relaxation time. Each compound (or tissue) has a characteristic T_1 that reflects the time required for signal recovery after an excitation pulse. Thus a shorter T_1, as caused by a T_1 contrast agent, results in faster signal recovery and therefore a brighter (hyperintense) region in the image. Gd^{3+} is the most commonly used T_1 agent. The ion has seven unpaired electrons and is consequently paramagnetic. For use *in vivo*, most of these unpaired electrons are bound by chelators to reduce the toxicity associated with free Gd^{3+} ions. A commonly used chelator is diethylene triamine pentaacetic acid (DTPA). Mn^{2+} is also used as a T_1 agent, especially for the detection of liver metastases. Similar to Gd-DPTA, Mn^{2+} is chelated to dipyroxyl diphosphate to reduce toxicity. The remaining sites on the Gd or Mn ions are available for coordination with water molecules; direct interaction with the water protons results in a decrease in T_1 at low concentrations of Gd or Mn, leading to localized regions of hyperintensity. Sequestration of the contrast agent in different cellular compartments or outside the cell in the extracellular matrix can affect

NIH-PA Author Manuscript

NIH-PA Author Manuscript

NIH-PA Author Manuscript

access to water and, in turn, the extent of their effect on image contrast. Finally, these agents can be toxic, for example Gd-based agents are associated with nephrogenic systemic fibrosis, although the mechanism is unknown [63].

T_2 and T_2* agents

T_2 is the transverse or spin-spin relaxation time. This time constant governs the decay of signal in the transverse plane. Acceleration of this signal loss by T_2 agents results in a localized dark (hypointense) spot due to the large magnetic field inhomogeneities they create (T_2* relaxation). These contrast agents can exert their effect over a larger radius than T_1 agents, and they also reduce T_2 and T_1. Superparamagnetic iron oxide (SPIO) is one of the most commonly used MRI contrast agents. Particulate SPIOs are categorized by size into ultra small (<50 nm, USPIOs), up to 1 μm (SPIOs), and >1 μm (micron-sized, or MPIOs). Some SPIO agents are in clinical use, which is beyond the scope of this article, but is reviewed in greater detail by [64].

Box 2. General requirements for an "ideal" ^{19}F label for cell tracking using MRI

The following list comprises the general requirements for a ^{19}F-based cell tracking label. In practice, the formulation is often a compromise of several of these factors. Cell label formulation is discussed further in Box 3.

1. The ^{19}F compound must be biologically inert and chemically stable. Fluorine is one of the most reactive elements and could wreak havoc in cells if free fluoride radicals were to form.
2. The ^{19}F compound must be stable in aqueous environments. Perfluorinated compounds are generally immiscible with water.
3. Cytotoxicity and any effect on cell function must be minimal. This applies to the ^{19}F compound and all other components of the formulation, such as surfactants.
4. The formulation of the label should be suitable for cell labeling. For example, intracellular labels may need to be small (~100 nm), while blood pool agents can be larger.
5. Cell uptake must be sufficient for detection, even by non-phagocytic cells. Cell uptake considerations also affect the choice of surfactant used, as these could modulate uptake based on their affinity for cell receptors or other biomolecules.
6. High ^{19}F density per molecule is often desirable, as it allows for a large accumulation of ^{19}F per voxel. Perfluorocarbons of relatively high molecular weight with a larger number of fluorine atoms, for example, would result in higher signal density per molecule. An alternative approach is to use a larger number of small fluorocarbons.
7. A single dominant resonance in the ^{19}F NMR spectrum is desirable to avoid chemical shift artifacts ("ghosts") caused by neighboring resonance peaks. The requirement for a single resonance also affects the surfactant or any compounds used in conjunction with the label (i.e. these surfactants or added compounds cannot contain fluorine). However, imaging techniques can be used to overcome the effect of multiple resonances; for example, much work has been done on correcting the chemical shift artifact in ^{19}F MR images of perfluorooctyl bromide (PFOB) [65,66]. MRS can exploit other parameters including scalar coupling, chemical exchange and relaxation processes [67]. Furthermore, the broad chemical shift range of ^{19}F allows the selection of fluorocarbons with sufficiently different

NIH-PA Author Manuscript

NIH-PA Author Manuscript

NIH-PA Author Manuscript

NMR resonances for multi-spectral imaging, where the two labels can be differentiated in a ^{19}F image, analogous to the simultaneous use of two non-overlapping fluorophores.

8. The ^{19}F compound must have favorable relaxation parameters. In general, this means a short T_1 and preferably a long T_2. Fluorinated block copolymers have been suggested as an alternative to PFCs [68]. Furthermore, some fluorinated compounds are oxygen-sensitive [69], which needs to be considered for quantification of cell numbers *in vivo*.

Box 3. ^{19}F label design and formulation

MRI labels for cell tracking are either contrast agents (primarily SPIO), or fluorinated compounds for ^{19}F MRI. While contrast agents function by modifying contrast locally, ^{19}F agents are somewhat like a “second color” and are often overlaid on the corresponding (grayscale) ^{1}H image used for anatomical localization, thus adding a second layer of independent information. ^{19}F labels or tracers are not contrast agents, and do not affect contrast in an anatomical ^{1}H image. Box 2 briefly describes the general characteristics of an “ideal” ^{19}F label. Formulation of a suitable label is often customized towards its intended application. Here, we focus on the use of PFC-based emulsions as these are currently the most widely used ^{19}F cell labels.

Once a suitable ^{19}F compound - or mixture of compounds - is selected, the compound needs to be stabilized in aqueous environments. The most thermodynamically stable state of two immiscible liquids, such as a PFC and water, is in two separate phases where the contact surface area between the two liquids is minimized. Hence, the formation of droplets, where the contact surface is greatly increased, requires the input of energy. Surfactants reduce this energy requirement, acting as an intermediary between the continuous and dispersed phases. As such, a fluorinated surfactant would be ideal, although this may affect the NMR properties of the label. Regardless, high molecular weight PFCs are difficult to solubilize and therefore necessitate high energy inputs, which can be achieved through the use of probe sonication or microfluidization, for example. The surfactants typically used in PFC emulsions for *in vivo* use include phospholipids [36,38,52,53,70] and pluronics [37,39, 40]. Phospholipids, such as lecithin, are generally considered to be safe. Some pluronics, such as F-68, are approved for human use. Other pluronics, such as L-61, are known to form channels in the cell membrane, and are being studied as chemosensitizing agents [71]. *In vivo*, pluronics are metabolized and excreted through urine and thus readily cleared from the system [72].

PFC emulsions generally age through Ostwald ripening, which results in the growth of larger droplets with a concurrent loss in smaller droplets. The high interfacial energy, high density of the fluorous dispersed phase, and the weak interactions between PFCs and water all contribute to emulsion instability [73]. Emulsions that might coagulate *in vivo* can result in acute toxicity, which was a major problem in the early development of PFC-based blood substitutes. However, since the low doses and mode of administration are completely different for intracellular labels, coagulation is less of a concern.

The main characteristics of an intracellular PFC label are a suitable PFC present at high concentrations in a manner suitable for cell uptake. Intracellular labels have been developed using microfluidization and perfluoro-15-crown-5 ether and lecithin surfactants [36], probe sonication and a Pluronic L-35 surfactant using a linear PFC [37,39], and microfluidization and linear PFCs [32,38,40,52]. Other fluorinated compounds are also being actively developed, including fluorinated dendrimers for ^{19}F MRI and drug delivery [74].

NIH-PA Author Manuscript

NIH-PA Author Manuscript

NIH-PA Author Manuscript

PFC emulsions from Celsense Inc. (Pittsburgh, PA) are currently being developed for cell tracking in the clinic [41]. Another area of interest in this field is the development of labels with a direct linkage [40] between the PFC and a dye or other agents, thereby ensuring that the groups are detected together. Extensive work on targeted agents for cellular MRI has also been carried out, where some have incorporated PFC, although detection primarily utilizes ^{1}H contrast agents [26-28].

Acknowledgments

We thank Dr. F. Bonetto for a critical reading of the manuscript, and Prof. D.H. Laidlaw for the description of the *in vivo* quantification technique. This research was supported by investment grants NWO middelgroot 40-00506-90-0602 and NWO BIG (VISTA) to AH; and the EU grants ENCITE (HEALTH-F5-2008-201842) and Cancerimmunotherapy (LSHC-CT-2006-518234), and NWO Vidi grant 917.76.363 to IJMdV. ETA acknowledges support from the National Institutes of Health (R01-CA134633, R01-EB003453, P01-HD047675, P41-EB001977) and the Dana Foundation.

References

1. Lucignani G, et al. Molecular imaging of cell-mediated cancer immunotherapy. Trends Biotechnol 2006;24:410–418. [PubMed: 16870284]
2. de Vries IJ, et al. Magnetic resonance tracking of dendritic cells in melanoma patients for monitoring of cellular therapy. Nat Biotechnol 2005;23:1407–1413. [PubMed: 16258544]
3. Bulte JW. In vivo MRI cell tracking: clinical studies. AJR Am J Roentgenol 2009;193:314–325. [PubMed: 19620426]
4. Himmelreich U, Dresselaers T. Cell labeling and tracking for experimental models using magnetic resonance imaging. Methods 2009;48:112–124. [PubMed: 19362150]
5. Gilad AA, et al. Developing MR reporter genes: promises and pitfalls. NMR Biomed 2007;20:275–290. [PubMed: 17451181]
6. Calamante F, et al. Contrast agent concentration measurements affecting quantification of bolus-tracking perfusion MRI. Magn Reson Med 2007;58:544–553. [PubMed: 17763347]
7. Liu W, Frank JA. Detection and quantification of magnetically labeled cells by cellular MRI. Eur J Radiol 2009;70:258–264. [PubMed: 18995978]
8. Arbab AS, et al. Cellular magnetic resonance imaging: current status and future prospects. Expert Rev Med Devices 2006;3:427–439. [PubMed: 16866640]
9. Goulle JP, et al. MRI gadolinium-based contrast agents. Radiologists beware! Ann Pharm Fr 2009;67:335–339. [PubMed: 19695369]
10. Nelson TR, et al. Fluorine nuclear magnetic resonance: calibration and system optimization. Magn Reson Imaging 1985;3:267–273. [PubMed: 4079674]
11. Holland GN, et al. 19F magnetic resonance imaging. Journal of Magnetic Resonance (1969) 1977;28:133–136.
12. Tran TD, et al. Clinical applications of perfluorocarbon nanoparticles for molecular imaging and targeted therapeutics. Int J Nanomedicine 2007;2:515–526. [PubMed: 18203420]
13. Simberg D, Mattrey R. Targeting of perfluorocarbon microbubbles to selective populations of circulating blood cells. J Drug Target 2009;17:392–398. [PubMed: 19505207]
14. Rapoport N, et al. Multifunctional nanoparticles for combining ultrasonic tumor imaging and targeted chemotherapy. J Natl Cancer Inst 2007;99:1095–1106. [PubMed: 17623798]
15. Diaz-Lopez R, et al. Liquid perfluorocarbons as contrast agents for ultrasonography and (19)F-MRI. Pharm Res 2010;27:1–16. [PubMed: 19902338]
16. Moriyasu F, Itoh K. Efficacy of perflubutane microbubble-enhanced ultrasound in the characterization and detection of focal liver lesions: phase 3 multicenter clinical trial. AJR Am J Roentgenol 2009;193:86–95. [PubMed: 19542399]
17. Soman N, Banerjee R. Artificial vitreous replacements. Biomed Mater Eng 2003;13:59–74. [PubMed: 12652023]

NIH-PA Author Manuscript

NIH-PA Author Manuscript

NIH-PA Author Manuscript

18. Lanza GM, et al. 1H/19F magnetic resonance molecular imaging with perfluorocarbon nanoparticles. Curr Top Dev Biol 2005;70:57–76. [PubMed: 16338337]
19. Lanza GM, et al. Targeted antiproliferative drug delivery to vascular smooth muscle cells with a magnetic resonance imaging nanoparticle contrast agent: implications for rational therapy of restenosis. Circulation 2002;106:2842–2847. [PubMed: 12451012]
20. Noth U, et al. 19F-MRI in vivo determination of the partial oxygen pressure in perfluorocarbon-loaded alginate capsules implanted into the peritoneal cavity and different tissues. Magn Reson Med 1999;42:1039–1047. [PubMed: 10571925]
21. Thomas SR, et al. Perfluorocarbon compound aerosols for delivery to the lung as potential 19F magnetic resonance reporters of regional pulmonary pO2. Invest Radiol 1997;32:29–38. [PubMed: 9007645]
22. Langereis S, et al. A temperature-sensitive liposomal 1H CEST and 19F contrast agent for MR image-guided drug delivery. J Am Chem Soc 2009;131:1380–1381. [PubMed: 19173663]
23. Mancini L, et al. A novel technique to monitor carboxypeptidase G2 expression in suicide gene therapy using 19F magnetic resonance spectroscopy. NMR Biomed 2009;22:561–566. [PubMed: 19259950]
24. Yu J, et al. Synthesis and evaluation of a novel gene reporter molecule: detection of beta-galactosidase activity using 19F NMR of a fluorinated vitamin B6 conjugate+ Med Chem 2005;1:255–262. [PubMed: 16787321]
25. Flogel U, et al. In vivo monitoring of inflammation after cardiac and cerebral ischemia by fluorine magnetic resonance imaging. Circulation 2008;118:140–148. [PubMed: 18574049]
26. Kaneda MM, et al. Perfluorocarbon Nanoemulsions for Quantitative Molecular Imaging and Targeted Therapeutics. Ann Biomed Eng. 2009
27. Moore A, et al. Tracking the recruitment of diabetogenic CD8+ T-cells to the pancreas in real time. Diabetes 2004;53:1459–1466. [PubMed: 15161749]
28. Morawski AM, et al. Quantitative “magnetic resonance immunohistochemistry” with ligand-targeted (19)F nanoparticles. Magn Reson Med 2004;52:1255–1262. [PubMed: 15562481]
29. Shapiro EM, et al. Magnetic resonance imaging of the migration of neuronal precursors generated in the adult rodent brain. Neuroimage 2006;32:1150–1157. [PubMed: 16814567]
30. Arbab AS, et al. Intracytoplasmic tagging of cells with ferumoxides and transfection agent for cellular magnetic resonance imaging after cell transplantation: methods and techniques. Transplantation 2003;76:1123–1130. [PubMed: 14557764]
31. Arbab AS, et al. Efficient magnetic cell labeling with protamine sulfate complexed to ferumoxides for cellular MRI. Blood 2004;104:1217–1223. [PubMed: 15100158]
32. Walczak P, et al. Instant MR labeling of stem cells using magnetoelectroporation. Magn Reson Med 2005;54:769–774. [PubMed: 16161115]
33. Zhao M, et al. Differential conjugation of tat peptide to superparamagnetic nanoparticles and its effect on cellular uptake. Bioconjug Chem 2002;13:840–844. [PubMed: 12121140]
34. Ahrens ET, et al. Receptor-mediated endocytosis of iron-oxide particles provides efficient labeling of dendritic cells for in vivo MR imaging. Magn Reson Med 2003;49:1006–1013. [PubMed: 12768577]
35. Bulte JW, et al. Magnetodendrimers allow endosomal magnetic labeling and in vivo tracking of stem cells. Nat Biotechnol 2001;19:1141–1147. [PubMed: 11731783]
36. Ahrens ET, et al. In vivo imaging platform for tracking immunotherapeutic cells. Nat Biotechnol 2005;23:983–987. [PubMed: 16041364]
37. Srinivas M, et al. Fluorine-19 MRI for visualization and quantification of cell migration in a diabetes model. Magn Reson Med 2007;58:725–734. [PubMed: 17899609]
38. Ruiz-Cabello J, et al. In vivo “hot spot” MR imaging of neural stem cells using fluorinated nanoparticles. Magn Reson Med 2008;60:1506–1511. [PubMed: 19025893]
39. Srinivas M, et al. In vivo cytometry of antigen-specific t cells using (19)F MRI. Magn Reson Med. 2009
40. Janjic JM, et al. Self-delivering nanoemulsions for dual fluorine-19 MRI and fluorescence detection. J Am Chem Soc 2008;130:2832–2841. [PubMed: 18266363]

NIH-PA Author Manuscript NIH-PA Author Manuscript NIH-PA Author Manuscript

41. Helfer BM, et al. Functional assessment of human dendritic cells labeled for in vivo(19)F magnetic resonance imaging cell tracking. Cytotherapy. 2010
42. Verdijk P, et al. Sensitivity of magnetic resonance imaging of dendritic cells for in vivo tracking of cellular cancer vaccines. Int J Cancer 2007;120:978–984. [PubMed: 17163419]
43. Mistretta CA. Undersampled radial MR acquisition and highly constrained back projection (HYPR) reconstruction: potential medical imaging applications in the post-Nyquist era. J Magn Reson Imaging 2009;29:501–516. [PubMed: 19243031]
44. Bornert P, et al. Fast perfluorocarbon imaging using 19F U-FLARE. Magn Reson Med 1993;29:226–234. [PubMed: 8429787]
45. Gowland PA, De Wilde J. Temperature increase in the fetus due to radio frequency exposure during magnetic resonance scanning. Phys Med Biol 2008;53:L15–18. [PubMed: 18843171]
46. Jager LJ, et al. Half-life of perfluorooctylbromide in inner organs determined by fast 19F-NMR imaging. Adv Exp Med Biol 1994;361:129–134. [PubMed: 7597935]
47. Noth U, et al. Fast 19F-NMR imaging in vivo using FLASH-MRI. Magn Reson Imaging 1994;12:149–153. [PubMed: 8295502]
48. Noth U, et al. In vivo measurement of partial oxygen pressure in large vessels and in the reticuloendothelial system using fast 19F-MRI. Magn Reson Med 1995;34:738–745. [PubMed: 8544695]
49. Weigel M, et al. Inversion recovery prepared turbo spin echo sequences with reduced SAR using smooth transitions between pseudo steady states. Magn Reson Med 2007;57:631–637. [PubMed: 17326168]
50. Ahrens ET, et al. Magnetic resonance imaging of embryonic and fetal development in model systems. Methods Mol Med 2006;124:87–101. [PubMed: 16506418]
51. Barber BJ, et al. Thermal effects of MR imaging: worst-case studies on sheep. AJR Am J Roentgenol 1990;155:1105–1110. [PubMed: 2120944]
52. Partlow KC, et al. 19F magnetic resonance imaging for stem/progenitor cell tracking with multiple unique perfluorocarbon nanobeacons. FASEB J 2007;21:1647–1654. [PubMed: 17284484]
53. Waters EA, et al. Detection of targeted perfluorocarbon nanoparticle binding using 19F diffusion weighted MR spectroscopy. Magn Reson Med 2008;60:1232–1236. [PubMed: 18956417]
54. Mattrey RF. The potential role of perfluorochemicals (PFCs) in diagnostic imaging. Artif Cells Blood Substit Immobil Biotechnol 1994;22:295–313. [PubMed: 8087248]
55. De Wilde JP, et al. A review of the current use of magnetic resonance imaging in pregnancy and safety implications for the fetus. Prog Biophys Mol Biol 2005;87:335–353. [PubMed: 15556670]
56. Tsai LL, et al. An open-access, very-low-field MRI system for posture-dependent 3He human lung imaging. J Magn Reson 2008;193:274–285. [PubMed: 18550402]
57. Kurhanewicz J, et al. Current and potential applications of clinical 13C MR spectroscopy. J Nucl Med 2008;49:341–344. [PubMed: 18322118]
58. Viale A, Aime S. Current concepts on hyperpolarized molecules in MRI. Curr Opin Chem Biol 2010;14:90–96. [PubMed: 19913452]
59. Flaim SF. Pharmacokinetics and side effects of perfluorocarbon-based blood substitutes. Artif Cells Blood Substit Immobil Biotechnol 1994;22:1043–1054. [PubMed: 7849908]
60. Millard RW. Oxygen solubility, rheology and hemodynamics of perfluorocarbon emulsion blood substitutes. Artif Cells Blood Substit Immobil Biotechnol 1994;22:235–244. [PubMed: 8087245]
61. Zarif L, et al. Biodistribution and excretion of a mixed fluorocarbon-hydrocarbon “dowel” emulsion as determined by 19F NMR. Artif Cells Blood Substit Immobil Biotechnol 1994;22:1193–1198. [PubMed: 7849922]
62. Olsen GW, et al. Perfluoroalkyl chemicals and human fetal development: an epidemiologic review with clinical and toxicological perspectives. Reprod Toxicol 2009;27:212–230. [PubMed: 19429401]
63. Natalin RA, et al. Contemporary applications and limitations of magnetic resonance imaging contrast materials. J Urol 2010;183:27–33. [PubMed: 19913804]
64. Geraldes CF, Laurent S. Classification and basic properties of contrast agents for magnetic resonance imaging. Contrast Media Mol Imaging 2009;4:1–23. [PubMed: 19156706]

NIH-PA Author Manuscript

NIH-PA Author Manuscript

NIH-PA Author Manuscript

65. Lee HK, et al. Correction for chemical-shift artifacts in 19F imaging of PFOB: simultaneous multislice imaging. Magn Reson Med 1991;21:21–29. [PubMed: 1943676]

66. Lee HK, et al. Correction of chemical-shift artifacts in 19F imaging of PFOB: a robust signed magnitude method. Magn Reson Med 1992;23:254–263. [PubMed: 1549040]

67. Yu JX, et al. 19F: a versatile reporter for non-invasive physiology and pharmacology using magnetic resonance. Curr Med Chem 2005;12:819–848. [PubMed: 15853714]

68. Peng H, et al. Synthesis and evaluation of partly fluorinated block copolymers as MRI imaging agents. Biomacromolecules 2009;10:374–381. [PubMed: 19128056]

69. Kodibagkar VD, et al. Physical principles of quantitative nuclear magnetic resonance oximetry. Front Biosci 2008;13:1371–1384. [PubMed: 17981636]

70. Neubauer AM, et al. Gadolinium-modulated 19F signals from perfluorocarbon nanoparticles as a new strategy for molecular imaging. Magn Reson Med 2008;60:1066–1072. [PubMed: 18956457]

71. Krylova OO, Pohl P. Ionophoric activity of pluronic block copolymers. Biochemistry 2004;43:3696–3703. [PubMed: 15035640]

72. Grindel JM, et al. Distribution, metabolism, and excretion of a novel surface-active agent, purified poloxamer 188, in rats, dogs, and humans. J Pharm Sci 2002;91:1936–1947. [PubMed: 12210041]

73. Yoon JK, Burgess DJ. Interfacial properties as stability predictors of lecithin-stabilized perfluorocarbon emulsions. Pharm Dev Technol 1996;1:333–341. [PubMed: 9552317]

74. Criscione JM, et al. Self-assembly of pH-responsive fluorinated dendrimer-based particulates for drug delivery and noninvasive imaging. Biomaterials 2009;30:3946–3955. [PubMed: 19443028]

NIH-PA Author Manuscript

NIH-PA Author Manuscript

NIH-PA Author Manuscript

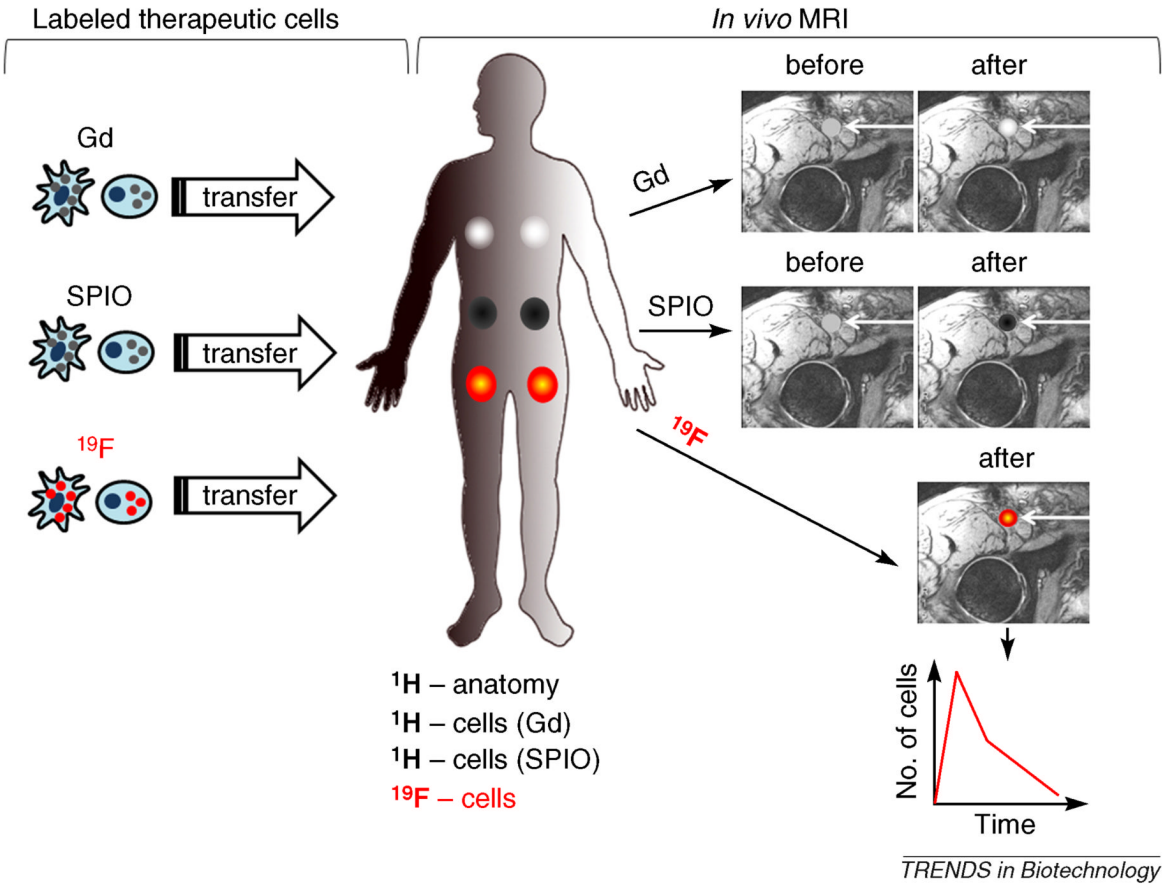

Figure 1.

Cell tracking using MRI with contrast agents and ^{19}F labels. Therapeutic cells (e.g. dendritic cells or stem cells) are labeled using contrast agents (Gd or SPIO), or a ^{19}F label. Conversely, typical anatomical MRI utilizes the ^{1}H from H_2O in tissues. Labeled cells are transferred to the patient by localized transfers, including intradermal or intranodal injections; the patient is then imaged to determine cell localization. Gd and SPIO (superparamagnetic iron oxide) labels typically require "before" and "after" images for localization (white arrows), resulting in a final hyperintense or hypointense spot signal, respectively. With a ^{19}F label, imaging can be carried out in a longitudinal manner for ^{19}F (specifically the labeled cells) and ^{1}H (anatomy) without a "before" image. Furthermore, the total ^{19}F signal can be calculated from the *in vivo* data, providing tracking information for both the localization and number of cells. Such quantitative, unambiguous cell tracking is not possible using standard imaging techniques in conjunction with metal-based contrast agents.

NIH-PA Author Manuscript

NIH-PA Author Manuscript

NIH-PA Author Manuscript

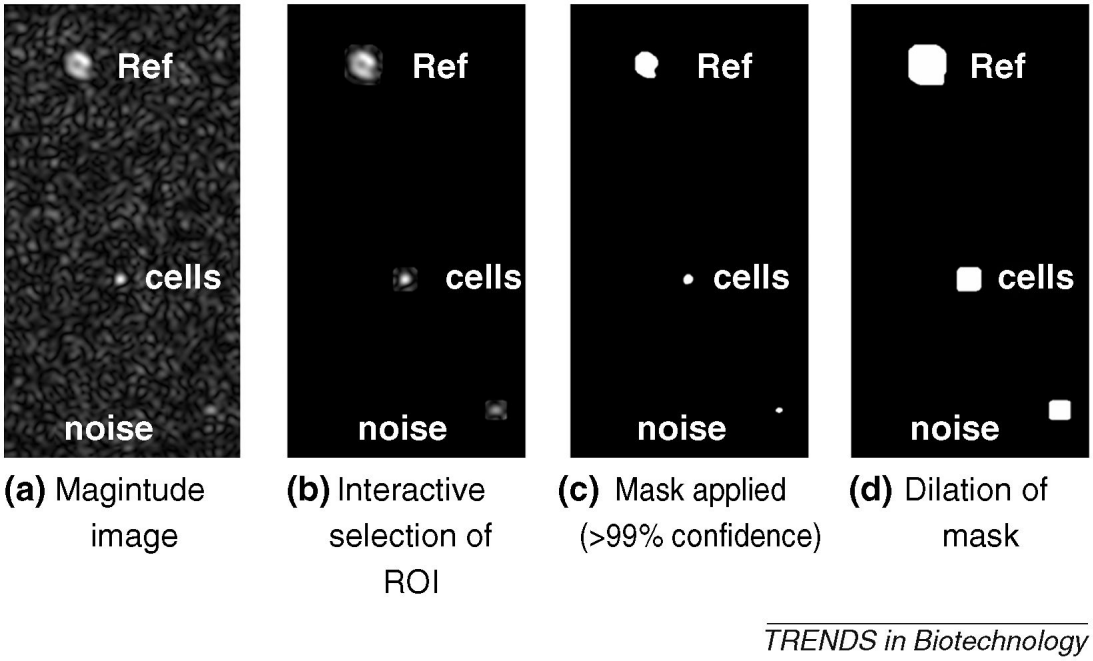

Figure 2.

Quantifying cell numbers directly from *in vivo* ^{19}F MR images, as described by [37]. (a, b) The magnitude ^{19}F image is manually processed for a selection of an ROI over the reference ('Ref'), which contains a known number of ^{19}F atoms per voxel), over the cells ('cells') and the background outside the subject ('noise'). (c) Next, a mask is applied to select only those voxels with signal greater than the noise with 99% confidence, after correction for Rician noise, when applicable. (d) The mask is then dilated by one-half a voxel in-plane to correct for partial volume effects. Finally, the total signal in the ROI over the cells is compared with that of the reference, and the number of ^{19}F atoms can then be calculated. Figure adapted from PhD thesis (M. Srinivas, Carnegie Mellon University, 2008).

NIH-PA Author Manuscript
NIH-PA Author Manuscript
NIH-PA Author Manuscript

Table 1

Summary of MRI cell labeling agents

Agent	Detection	Image effect	Sensitivity	Quantification	Toxicity
Iron oxide (FeO, Fe_2O_3, Fe_3O_4)	T_2*	Hypointensity	+++	+	++
Gd^{3+}, Mn^{2+}	T_1	Hyperintensity	++	+	+++
^{19}F	spin density	Presence or absence	+	+++	+